Radiative jet energy loss in a three-dimensional hydrodynamical medium and high p_T azimuthal asymmetry of π_0 suppression at mid and forward rapidity at RHIC

Guang-You Qin,[1] Jörg Ruppert,[1] Simon Turbide,[1] Charles Gale,[1] Chiho Nonaka,[2] and Steffen A. Bass[3]

[1]*Department of Physics, McGill University, Montreal, Quebec, H3A 2T8, Canada*
[2]*Department of Physics, Nagoya University, Nagoya 464-8602, Japan*
[3]*Department of Physics, Duke University, Durham, NC 27708, USA*

(Dated: February 1, 2008)

The nuclear modification factor R_{AA} for π_0 production in Au+Au collisions at $\sqrt{s} = 200$ AGeV is calculated, and studied at high transverse momenta p_T. The soft thermalized nuclear medium is described within the framework of relativistic ideal three-dimensional hydrodynamics. The energy loss of partonic jets is evaluated in the context of gluon bremsstrahlung in the thermalized partonic matter. We provide a systematic analysis of the azimuthal asymmetry of π_0 suppression at high p_T in central and non-central collisions, at mid and forward rapidity. The determination of R_{AA} as a function of p_T, at different azimuthal angles, and different rapidities makes for a stringent test of our theoretical understanding of jet energy loss over a variety of in-medium path lengths, temperatures and initial partonic jet energies. This lays the groundwork for a tomography of the nuclear medium.

I. INTRODUCTION

Experiments at the Relativistic Heavy Ion Collider (RHIC) have shown that high p_T hadrons in central A+A collisions are significantly suppressed in comparison with those in binary p+p interactions, scaled to nucleus-nucleus collisions [1, 2]. This phenomenon is commonly attributed to the fact that partonic jets produced in the early pre-equilibrium stage of the collisions interact with the hot and dense nuclear medium created in those collisions and loose energy in the process. This is referred to as *jet-quenching* [3]. These lower energy partonic jets traverse the medium and will eventually fragment into hadrons which are observed in the detectors.

Theoretical formalisms have been elaborated to describe the energy loss following the gluon bremsstrahlung experienced by the color charges in the medium: we mention the work by Baier-Dokshitzer-Mueller-Peigne-Schiff (BDMPS) [4], Gyulassy-Levai-Vitev (GLV) [5], Kovner-Wiedemann (KW) [6], Zakharov [7], Majumder-Wang-Wang (Higher Twist) [8], and Arnold-Moore-Yaffe (AMY) [9].

Recent studies [10, 11, 12] indicate that additional collisional energy loss of light partons might be substantial as well. However, a consistent treatment including (possibly destructive) interference is to be developed [13]. In this article we will restrict ourselves to the calculation of energy loss of the hard partons induced by gluon bremsstrahlung in the deconfined phase.

Jet quenching can be experimentally quantified by measurements of various quantities as e.g. the nuclear modification factor R_{AA}, the elliptic flow v_2 at high p_T, and high p_T hadron correlations. While considerable theoretical effort has been deployed to develop and improve our understanding of modifications of jets in the nuclear medium, early jet quenching calculations often relied on an elementary description of the soft medium in their description of data. In most works the jets traverse a simple density distribution which varies with time unconstrained by the bulk observables, with or without a Bjorken expansion, see e.g. [14, 15]. Similarly, calculations estimating the effects of three dimensional (3D) expansion on R_{AA} have treated the energy loss of jets in a simplified fashion [16].

In [17] a parameterized non-Bjorken fireball evolution that accounts for several measured observables connected with bulk properties of the matter created at RHIC [18] was applied to study the effect of flow on energy loss (in the BDMPS formalism, according to the prescription outlined in [19]). This study aimed for a sophisticated description of energy loss as well as for the medium evolution, but it was restricted to the calculation of R_{AA} in central collisions. Later this observable was also studied in a 2D hydrodynamical evolution model [20]. Recently, a 3D hydrodynamical evolution calculation [21] of the expanding medium in central and non-central collisions was employed in detailed studies of jet energy loss as predicted in the BDMPS formalism [22, 23] and in the higher twist formalism [24].

The present work contributes to this effort of understanding the physics of jet quenching by applying the Arnold, Moore, and Yaffe (AMY) formalism [9] for gluon bremsstrahlung to calculate the jet energy loss in the thermal partonic medium in central and non-central collision as inferred from 3D relativistic hydrodynamics [21]. We present a calculation of R_{AA} as a function of transverse momentum (and the azimuth) in central and non-central collisions and also study the rapidity dependence of this quantity.

While R_{AA} as measured in central collisions *alone* is not suited to distinguish in detail between different theoretical conjectures about jet energy loss [25], the combination with additional measurements of R_{AA} versus reaction plane in non-central collisions [26] and at finite rapidity provides further valuable tomographic information. Additional tomographic observables are high p_t triggered correlation measurements, see e.g. [20, 27, 28].

The paper is organized as follows, we first briefly re-

view the 3D hydrodynamical description of the medium in Sec. II. We then discuss in Sec. III how the initial momentum distributions of jets and their time-evolution in the thermal medium (which incorporates the energy loss process in the AMY formalism) as well as the fragmentation of the final jets into pions are calculated. Numerical results are presented for R_{AA} at mid and forward rapidity in Sec. IV together with a comparison to data where already available. Finally, Sec. V contains our conclusions.

II. 3D HYDRODYNAMICAL MEDIUM

The behavior related to the bulk properties of the high-density phase in heavy-ion collisions at RHIC is well described by Relativistic Fluid Dynamics (RFD, see e.g. [29, 30, 31]), while this description is not applicable in the late dilute stages of the collisions in which the mean free path of hadrons is large on the typical scales of the system.

In the present paper we use a fully 3D hydrodynamical model for the description of RHIC physics [21] which solves the relativistic hydrodynamical equation

$$\partial_\mu T^{\mu\nu} = 0, \tag{1}$$

where $T^{\mu\nu}$ is the energy momentum tensor which can be expressed as

$$T^{\mu\nu} = (\epsilon + p)U^\mu U^\nu - p g^{\mu\nu}. \tag{2}$$

Here ϵ, p, U and $g^{\mu\nu}$ are energy density, pressure, four velocity and metric tensor, respectively. Furthermore baryon number n_B conservation is imposed as a constraint

$$\partial_\mu (n_B(T,\mu)U^\mu) = 0, \tag{3}$$

and the resulting set of partial differential equations is closed by specifying an equation of state (EoS): $\epsilon = \epsilon(p)$. Our particular RFD calculation utilizes a Lagrangian mesh and the coordinates (τ, x, y, η) with the longitudinal proper time $\tau = \sqrt{t^2 - z^2}$ and space-time rapidity $\eta = \frac{1}{2}\ln[(t+z)/(t-z)]$ in order to optimize the calculation for the ultra-relativistic regime of heavy collisions at RHIC. Once an initial condition has been specified RFD in the ideal fluid approximation (i. e. neglecting off-equilibrium effects) allows a calculation of single soft matter properties at RHIC, especially collective flow and particle spectra.

We assume early thermalization with subsequent hydrodynamical expansion at $\tau_0 = 0.6$ fm/c. The initial conditions, namely initial energy density and baryon number density are parameterized by

$$\begin{aligned} \epsilon(x,y,\eta) &= \epsilon_{\max} W(x,y;b) H(\eta), \\ n_B(x,y,\eta) &= n_{B\max} W(x,y;b) H(\eta), \end{aligned} \tag{4}$$

where b and $\epsilon_{\max}$ ($n_{B\max}$) are the impact parameter and the maximum value of energy density (baryon number density), respectively. $W(x,y;b)$ is given by a combination of wounded nucleon model and binary collision model [32] and $H(\eta)$ is given by $H(\eta) = \exp\left[-(|\eta| - \eta_0)^2/(2\sigma_\eta^2) \cdot \theta(|\eta| - \eta_0)\right]$.

The initial conditions have been chosen such that a successful description of the soft sector at RHIC (elliptic flow, pseudo-rapidity distributions and low-p_T single particle spectra) is achieved. For further details, especially also a discussion of the EoS which is employed, we refer the reader to [21].

III. JET EVOLUTION AND FRAGMENTATION

In this section we present the techniques used to calculate the initial jet production in the early stage of the collisions, the subsequent propagation through the hot and dense medium, and final hadronization in the vacuum. We exclusively focus on the hadrons in the high p_T region in which fragmentation is the dominant mechanism for the production of hadrons. For softer hadrons (below $p_T \sim 7$ GeV/c) other mechanisms, such as the recombination of partons become of increasing significance [33].

The initial jet density distribution $\mathcal{P}_{AB}(b, \vec{r}\perp)$ at the transverse position $\vec{r}_\perp$ and in A+B collisions with impact parameter $\vec{b}$ is given by

$$\mathcal{P}_{AB}(b, \vec{r}_\perp) = \frac{T_A(\vec{r}_\perp + \vec{b}/2) T_B(\vec{r}_\perp - \vec{b}/2)}{T_{AB}(b)}. \tag{5}$$

Here we use a Woods-Saxon form for the nuclear density function, $\rho(\vec{r}_\perp, z) = \rho_0/[1 + \exp(\frac{r-R}{d})]$, to evaluate the nuclear thickness function $T_A(\vec{r}_\perp) = \int dz \rho_A(\vec{r}_\perp, z)$ and the overlap function of two nuclei $T_{AB}(b) = \int d^2 r_\perp T_A(\vec{r}_\perp) T_B(\vec{r}_\perp + \vec{b})$. The values of the parameters $R = 6.38$ fm and $d = 0.535$ fm are taken from [34].

The initial momentum distribution $dN^j_{AB}(b)/d^2p^j_T dy|_i$ of jets is computed from pQCD in the factorization formalism,

$$\begin{aligned} \left.\frac{dN^j_{AB}(b)}{d^2p^j_T dy}\right|_i &= T_{AB}(b) \sum_{abd} \int dx_a G_{a/A}(x_a, Q) G_{b/B}(x_b, Q) \\ &\quad \times \frac{1}{\pi} \frac{2x_a x_b}{2x_a - x^j_T e^y} K \frac{d\sigma_{a+b\to j+d}}{dt}. \end{aligned} \tag{6}$$

In the above equation, $G_{a/A}(x_a, Q)$ is the distribution function of parton a with momentum fraction x_a in the nucleus A at factorization scale Q, taken from CTEQ5 [35] including nuclear shadowing effects from EKS98 [36]. The index j represents one of the partonic species ($j = q, \bar{q}, g$), and $x^j_T = 2p^j_T/\sqrt{s_{NN}}$, where $\sqrt{s_{NN}}$ is the center of mass energy. The distribution $d\sigma/dt$ is the leading order QCD differential cross section, and the K-factor accounts for NLO effects and is taken to be constant in our calculation as it is almost p_T independent [37, 38, 39]. The initial Cronin effect is neglected in our

calculation since the nuclear modification factor of neutral pions from d+Au collisions measured by PHENIX is consistent with 1 within systematic errors [40].

The evolution of a jet momentum distribution $P_j(p,t) = dN_j(p,t)/dpdy$ (essentially the probability of finding a jet with energy p at time t) in the medium is obtained in the AMY formalism by solving a set of coupled rate equations (for details see [41, 42]), which have the following generic form,

$$\frac{dP_j(p,t)}{dt} = \sum_{ab}\int dk\left[P_a(p+k,t)\frac{d\Gamma^a_{jb}(p+k,k)}{dkdt} - P_j(p,t)\frac{d\Gamma^j_{ab}(p,k)}{dkdt}\right], \quad (7)$$

where $d\Gamma^j_{ab}(p,k)/dkdt$ is the transition rate for the partonic process $j \to a+b$. We point out that the calculation includes not only the emission but also the absorption of thermal partons as the k integral in Eq. (7) ranges from $-\infty$ to ∞. The transition rate is given by [41, 42]

$$\frac{d\Gamma(p,k)}{dkdt} = \frac{C_s g_s^2}{16\pi p^7}\frac{1}{1\pm e^{-k/T}}\frac{1}{1\pm e^{-(p-k)/T}} \times \left\{\begin{array}{ll} \frac{1+(1-x)^2}{x^3(1-x)^2} & q\to qg \\ N_{\rm f}\frac{x^2+(1-x)^2}{x^2(1-x)^2} & g\to q\bar{q} \\ \frac{1+x^4+(1-x)^4}{x^3(1-x)^3} & g\to gg \end{array}\right\} \times \int\frac{d^2\vec{h}}{(2\pi)^2}2\vec{h}\cdot{\rm Re}\,\vec{F}(\vec{h},p,k)\,. \quad (8)$$

Here C_s is the quadratic Casimir relevant for the process, and $x \equiv k/p$ is the momentum fraction of the gluon (or the quark, for the case $g \to q\bar{q}$). $\vec{h} \equiv \vec{p}\times\vec{k}$ determines how non-collinear the final state is; it is treated as parametrically $O(g_s T^2)$ and therefore small compared to $\vec{p}\cdot\vec{k}$. Therefore it can be taken as a two-dimensional vector in transverse space. $\vec{F}(\vec{h},p,k)$ is the solution of the following integral equation [41, 42]:

$$2\vec{h} = i\delta E(\vec{h},p,k)\vec{F}(\vec{h}) + g_s^2\int\frac{d^2\vec{q}_\perp}{(2\pi)^2}C(\vec{q}_\perp) \times\Big\{(C_s - C_{\rm A}/2)[\vec{F}(\vec{h}) - \vec{F}(\vec{h}-k\,\vec{q}_\perp)] +(C_{\rm A}/2)[\vec{F}(\vec{h}) - \vec{F}(\vec{h}+p\,\vec{q}_\perp)] +(C_{\rm A}/2)[\vec{F}(\vec{h}) - \vec{F}(\vec{h}-(p-k)\,\vec{q}_\perp)]\Big\}. \quad (9)$$

Here $\delta E(\vec{h},p,k)$ is the energy difference between the final and the initial states:

$$\delta E(\vec{h},p,k) = \frac{\vec{h}^2}{2pk(p-k)} + \frac{m_k^2}{2k} + \frac{m_{p-k}^2}{2(p-k)} - \frac{m_p^2}{2p}\,, \quad (10)$$

and m^2 are the medium induced thermal masses. Also, $C(\vec{q}_\perp)$ is the differential rate to exchange transverse (to the parton) momentum $\vec{q}_\perp$. In a hot thermal medium, its value at leading order in $\alpha_{\rm s}$ is [43]

$$C(\vec{q}_\perp) = \frac{m_D^2}{\vec{q}_\perp^{\,2}(\vec{q}_\perp^{\,2}+m_D^2)}\,, \quad m_D^2 = \frac{g_s^2T^2}{6}(2N_{\rm c}+N_{\rm f})\,. \quad (11)$$

For the case of $g \to q\bar{q}$, $(C_s - C_{\rm A}/2)$ should appear as the prefactor on the term containing $\vec{F}(\vec{h} - p\,\vec{q}_\perp)$ rather than $\vec{F}(\vec{h} - k\,\vec{q}_\perp)$.

The strength of the transition rate in pQCD is controlled by the strong coupling constant α_s, temperature T and the flow parameter $\vec{\beta}$ (the velocity of the thermal medium) relative to the jet's path. In a 3D expanding medium, the transition rate is first evaluated in the local frame of the thermal medium, then boosted into the laboratory frame,

$$\left.\frac{d\Gamma(p,k)}{dkdt}\right|_{lab} = (1-\vec{v}_j\cdot\vec{\beta})\left.\frac{d\Gamma(p_0,k_0)}{dk_0dt_0}\right|_{local}, \quad (12)$$

where $k_0 = k(1-\vec{v}_j\cdot\vec{\beta})/\sqrt{1-\beta^2}$ and $t_0 = t\sqrt{1-\beta^2}$ are momentum and the proper time in the local frame, and $\vec{v}_j$ is the velocity of the jet. As jets propagate in the medium, the temperature and the flow parameter depend on the time and the positions of jets, and the 3D hydrodynamical calculation [21] is utilized to determine the temperature and flow profiles. The energy-loss mechanism is applied at $\tau_0 = 0.6$ fm/c, when the medium reaches thermal equilibrium, and turned off when the medium reaches the hadronic phase.

The final hadron spectrum $dN^h_{AB}(b)/d^2p_Tdy$ at high p_T is obtained by the fragmentation of jets in the vacuum after their passing through the 3D expanding medium,

$$\frac{dN^h_{AB}(b)}{d^2p_Tdy} = \sum_j\int d^2\vec{r}_\perp\mathcal{P}_{AB}(b,\vec{r}_\perp)\int\frac{dz_j}{z_j^2}D_{h/j}(z_j,Q_F) \times\left.\frac{dN^j_{AB}(b,\vec{r}_\perp)}{d^2p_T^jdy}\right|_f, \quad (13)$$

where $dN^j_{AB}(b,\vec{r}_\perp)/d^2p_T^jdy|_f$ is the final momentum distribution of the jet initially created at transverse position $\vec{r}_\perp$ after passing through the medium. The fragmentation function $D_{h/j}(z_j,Q_F)$ gives the average multiplicity of the hadron h with the momentum fraction $z_j = p_T/p_T^j$ produced from a jet j at a scale Q_F, taken from KKP parametrization [44]. The fractorization scale $Q = p_T^j$ and fragmentation scale $Q_F = p_T$ are set as in [37] where the K-factor is found to be 2.8. We use these values throughout the present study. This nicely reproduces the experimentally measured π_0 yield at mid and forward rapidity in p+p collisions at $\sqrt{s} = 200$ GeV, as shown in Fig. 1 and Fig. 2. It can be clearly seen that replacing the CTEQ5 parton distribution functions by MRST01 [46] yields essentially the same result for the inclusive π_0 production in p+p collisions. We point out that the presence of a nuclear medium might in principle alter these scales but we postpone a detailed study of this possibility to future research.

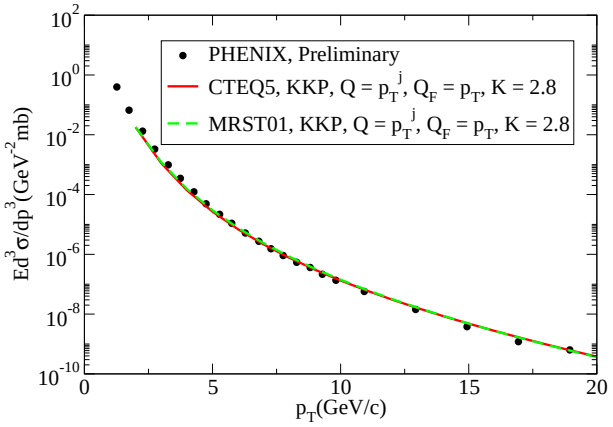

FIG. 1: (Color online) The inclusive cross section for π_0 production versus π_0 transverse momentum at mid-rapidity in pp collisions at $\sqrt{s} = 200$ GeV, compared with PHENIX data [45].

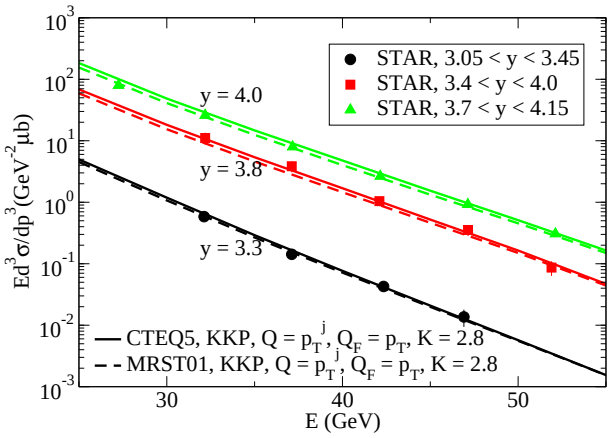

FIG. 2: (Color online) The inclusive cross section for π_0 production versus π_0 energy at forward rapidity in pp collisions at $\sqrt{s} = 200$ GeV. Data points are taken from STAR [47].

The nuclear modification factor R_{AA} is defined as the ratio of the hadron yield in A+A collisions to that in p+p interactions scaled by the number of binary collisions

$$R^h_{AA}(b, \vec{p}_T, y) = \frac{1}{N_{coll}(b)} \frac{dN^h_{AA}(b)/d^2p_T dy}{dN^h_{pp}/d^2p_T dy}. \quad (14)$$

IV. RESULTS

In Fig. 3, we present the calculation of the nuclear modification factor R_{AA} for neutral pions measured at midrapidity for two different impact parameters $b = 2.4$ fm and $b = 7.5$ fm, compared with (preliminary) PHENIX data for most central $(0 - 5\%)$ and midcentral $(20 - 30\%)$ collisions [26]. All results presented throughout the paper are for Au+Au collisions at $\sqrt{s} =$ 200 AGeV. We only show results for the nuclear modification factor R_{AA} for neutral pions, as results for charged hadrons (including contributions from charged pions, kaons and protons) are qualitatively similar.

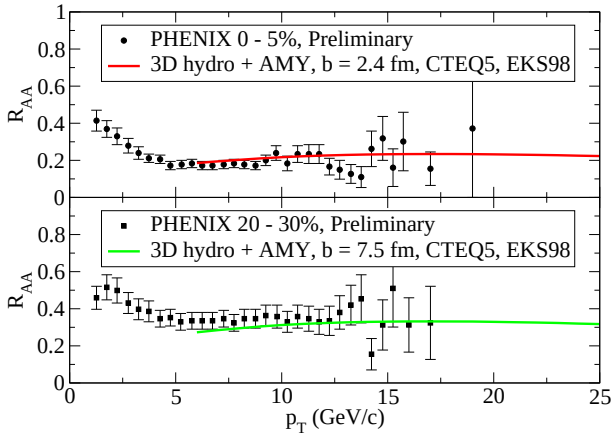

FIG. 3: (Color online) The neutral pion R_{AA} at midrapidity in most central (upper panel) and midperipheral (lower panel) Au+Au collisions compared with PHENIX data.

Once the temperature evolution is fixed by the initial conditions and subsequent 3D hydrodynamical expansion, the strong coupling constant α_s is the only quantity which is not uniquely determined in the model. The value of α_s is a direct measure of the interaction strength and is adjusted in such a way that the experimental data in the most central collisions is described. The same value, $\alpha_s = 0.33$, is used in peripheral collisions. Treating α_s as T-independent from early thermalization on down to the phase transition temperature is a simplification and corresponds to the assumption that the deconfined phase of the medium formed in Au+Au collisions at 200 AGeV at RHIC can be characterized by one average effective coupling. We point out that a treatment in the AMY formalism only considers energy loss in the partonic phase, hadronic energy loss is not included in the present study [49]. We have verified that choosing different constant values of α_s does not influence the shape of R_{AA} as a function of p_T significantly while only the overall normalization is affected. We point out that although $\alpha_s < 1$, $g_s = \sqrt{4\pi\alpha_s}$ is actually larger than 1. In that sense our study does not contradict the finding in [22] that a stronger quenching power of the medium has to be assumed than if a fully perturbative treatment of jet quenching in the quark gluon plasma is employed. (In [22] uncertainties in the selection of the strong coupling and possible non-perturbative effects were parameterized by a factor K in $\hat{q} = 2K\epsilon^{3/4}$. $K \approx 3.6$ was adjusted to give a good description of R_{AA} in central collisions at mid-rapidity.)

In Fig. 3, R_{AA} at midrapidity is averaged over the azimuth ϕ. More tomographic capabilities can be achieved if one studies R_{AA} at midrapidity in *non-central* colli-

sions not only as a function of p_T averaged over ϕ but also as a function of the azimuth ϕ [26].

The reason is that the initial geometric asymmetry in non-central collisions leaves its imprint on the 3D hydrodynamical evolution and initial jets experience different energy loss (depending on where they are produced in the medium and in which direction they are emitted) owing to the different local properties of the nuclear medium with which they interact. In the AMY formalism the important input from the evolution is the temperature in the rest frame of the local fluid that the jet experiences (and to a lesser extent the flow profile of the medium, as discussed later).

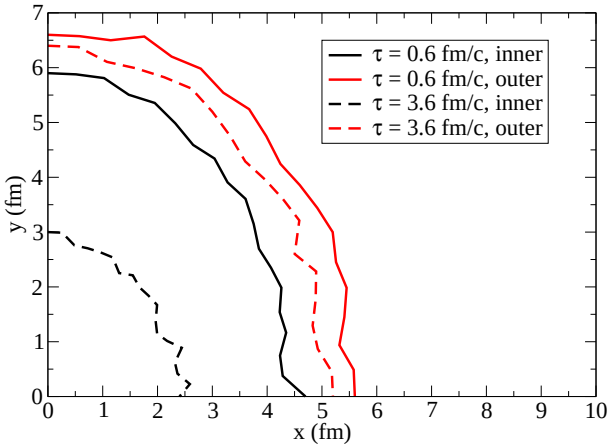

FIG. 4: (Color online) The inner and outer boundaries for $T = T_c$ in the transverse plane at two different proper times, $b = 7.5$ fm.

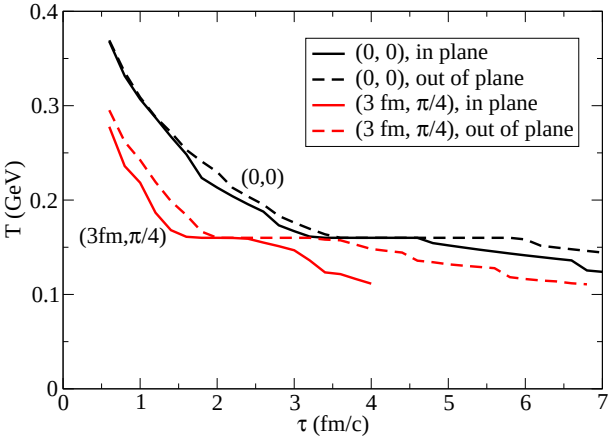

FIG. 5: (Color online) The time evolution of the temperature seen by a jet initially created at (r_0, ϕ_0) moving in plane and out of plane through the medium, $b = 7.5$ fm.

To illustrate the geometrical asymmetry we show in Fig. 4 isotherms for $T = T_c$ in the transverse plane for an impact parameter of $b = 7.5$ fm at two different proper times of the evolution. They represent the inner and outer boundaries of the mixed phase during the evolution. The geometric asymmetry of the temperature profile can be clearly seen from the plot. Both boundaries move towards the center and the inner boundary moves faster than the outer boundary. It is useful to define the emission in plane ($\phi = 0$) versus out of plane ($\phi = \pi/2$). We point out that the ratios of the boundary positions in plane to those out of plane are almost constant in proper time and have almost the same values for the inner and outer boundaries: ~ 0.8.

Fig. 5 shows the temperature observed by a jet traversing this medium. The jet is assumed to be created at position (r_0, ϕ_0) by a hard scattering at early times in the heavy-ion collision. As it propagates through the medium, the surrounding environment will change from the QGP phase to the mixed phase, then to the hadronic phase and will eventually freeze-out. We plot the temperature evolution experienced by jets that are created in a symmetric position ($\phi_0 = \pi/4$) relative to in-plane and out-of-plane and illustrate the geometrical asymmetry of the medium. We compare jets starting at the origin and those at $r = 3$ fm.

Jets that propagate out of plane will pass the mixed phase and the hadronic phase at later proper time than those traversing in plane and will interact with the deconfined and mixed phase of the medium longer. If the jets have identical initial energy, the energy loss experienced by the jets propagating out of plane will therefore be larger than in plane.

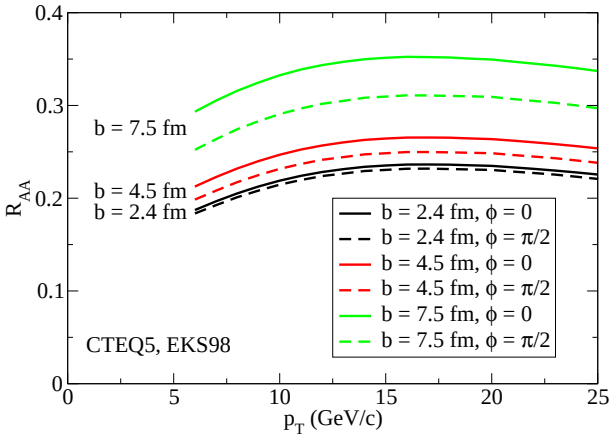

FIG. 6: (Color online) The neutral pion R_{AA} at midrapidity for emissions in plane and out of plane as a function of p_T for different impact parameters.

This behavior is reflected in R_{AA} as a function of p_T for emissions in plane and out of plane in Fig. 6 for different impact parameters. While there is very small difference for R_{AA} between the two planes in central collisions, a much larger difference for midcentral collisions (about 13% for $b = 7.5$ fm) is predicted, as can been seen from the ratio of R_{AA} for emission out of plane to that in plane

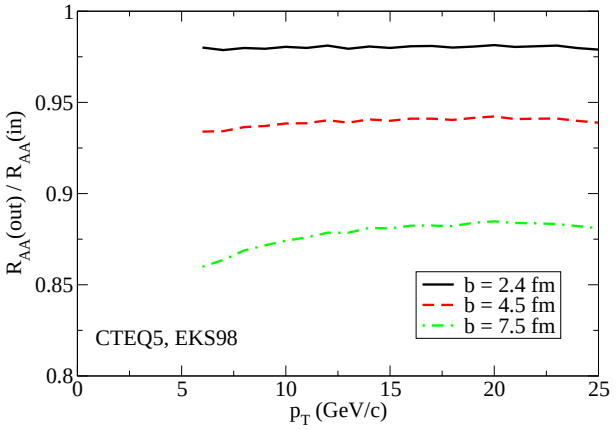

FIG. 7: (Color online) The ratio of the neutral pion R_{AA} at midrapidity for emissions in plane and out of plane as a function of p_T for different impact parameters.

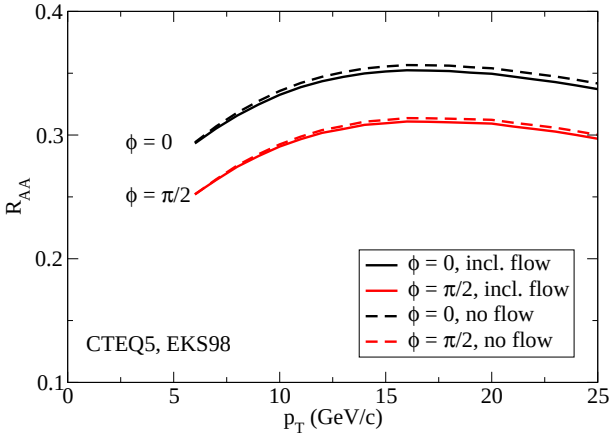

FIG. 9: (Color online) Comparing the neutral pion R_{AA} at midrapidity with and without flow for emissions in plane and out of plane as a function of p_T, $b = 7.5$ fm.

as shown in Fig. 7.

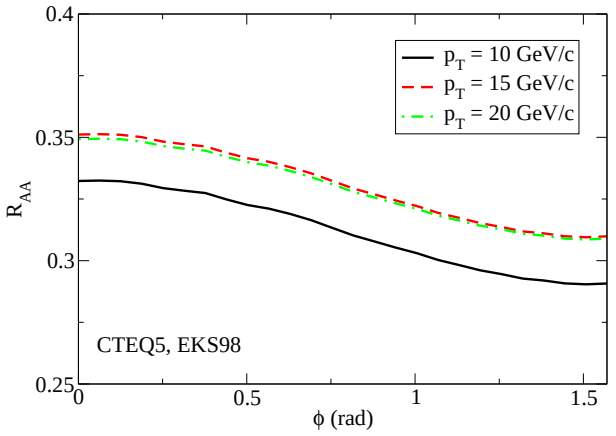

FIG. 8: (Color online) The neutral pion R_{AA} at midrapidity as a function of the azimuthal angle ϕ of the pion for different p_T, $b = 7.5$ fm.

As a further tomographic quantity, one can also study R_{AA} for non-central collisions as a function of the azimuthal angle ϕ for different p_T, see Fig. 8. A monotonous decrease of R_{AA} for emissions from in plane to out of plane, reflects (an average of) the asymmetric temperature (and flow) profiles experienced by the jets while they traverse the medium.

In a 3D expanding medium, there is also considerable collective flow being built up during the evolution. This can affect the energy loss of jets and may to some degree influence the asymmetry in the final pion spectrum. To quantify this effect, we use the same 3D hydro temperature profile, but disregard the transverse flow. We compare the case with flow to one where the velocity effect is disregarded, namely $\vec{\beta} = 0$ is enforced by hand in Eq. (12) (only for illustration purposes). This treatment can give an estimate on how collective flow (not the temperature of the medium) influences the jet energy loss in the evolution. As is shown in Fig. 9, flow effects only slightly increase the quenching power of the medium in the AMY-formalism. It is emphasized that for a realistic hydrodynamical calculation, the overall temperature of the medium would drop not as fast if collective flow was switched off and the medium itself would expand more slowly in this case.

We point out that a further interesting quantity is R_{AA} for neutral pions as a function of p_T at different centralities and away from midrapidity. The formalism as outlined in Section II. can be straightforwardly extended to treat this case. Caveats are that only moderate deviations from midrapidity can be allowed, because the nuclear parton distribution functions can be less exactly determined in the relevant region [36] and the assumption of a thermalized medium essential for a hydrodynamical treatment is no longer fulfilled far away from midrapidity. We therefore restrict our study to rapidities close to midrapidity (maximum forward rapidity $y = 2$).

At finite rapidity y the energy of a highly-relativistic jet with a transverse momentum p_T is given by $E = p_T \cosh y$. The pions at a fixed p_T have more energy and are the fragments of higher energetic partons than the corresponding midrapidity pions. The initial jet distribution of quarks and anti-quarks is shown in Fig. 10 for different rapidities, compare Eq. (6). Note that the kinematical cut off at $E = \sqrt{s_{NN}}/2 = 100$ GeV is reached at lower p_T for finite y.

In Fig. 11 we show R_{AA} as a function of p_T for central collisions ($0 - 5\%$, $b = 2.4$ fm) at mid and forward rapidity. It is interesting to notice that R_{AA} behaves quite differently as a function of p_T at $y = 2$ than at $y = 0$. This is not only due to the different temperature profiles of the hydrodynamical medium at forward rapidity but also strongly influenced by the different initial jet distri-

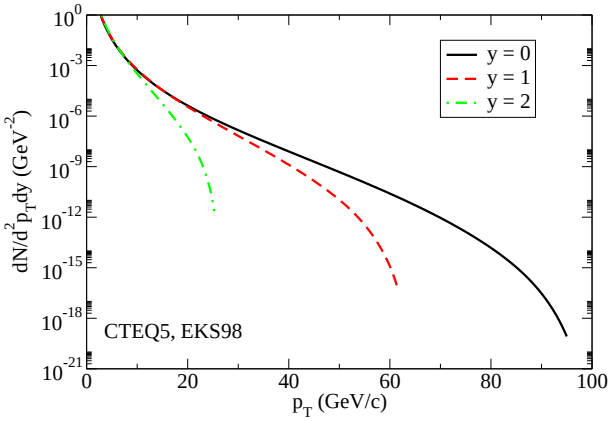

FIG. 10: (Color online) The jet (quark + anti-quark) transverse momentum distribution at different rapidities, b = 2.4 fm.

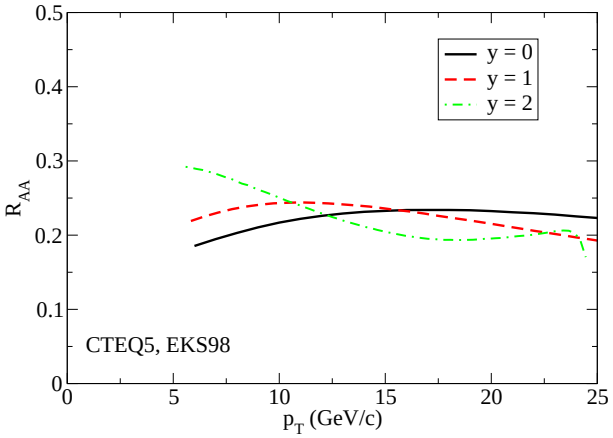

FIG. 11: (Color online) The neutral pion R_{AA} at different rapidities, $b = 2.4$ fm.

butions, see Fig. 10.

To provide additional insight, we studied the same quantity averaged over ϕ for midcentral collisions with an impact parameter of b = 7.5 fm with and without nuclear shadowing effects taken into account in the parton distribution functions utilized in Eq. (6). Results are shown in Fig. 12. It is interesting to notice that R_{AA} is not monotonously increasing as a function of p_T. The midrapidity R_{AA} is decreasing above $\sim$ 18 GeV/c (with nuclear shadowing), the turning point for $y = 1$ is at $\sim$ 9 GeV/c (with nuclear shadowing). The values of R_{AA} at $y = 2$ decreases monotonically above $\sim$ 6 GeV/c in the case without nuclear shadowing and exhibits two turning points if shadowing is taken into account. We have also found that assuming a simple power law approximation for dN/d^2p_Tdy distributions for all values of p_T would lead to increased R_{AA} at higher p_T (comparison not shown). This demonstrates that the overall decrease of R_{AA} at higher p_T is mainly due to the initial

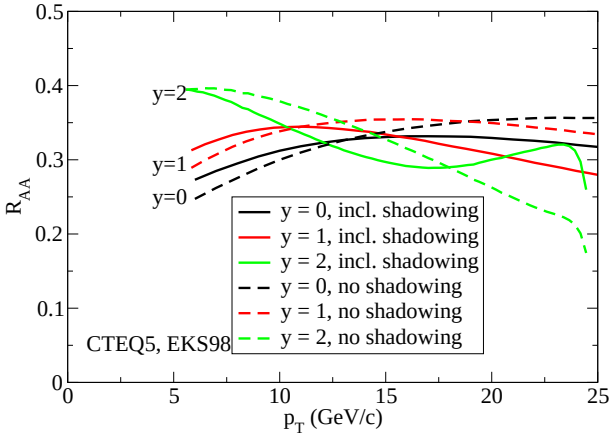

FIG. 12: (Color online) Comparing neutral pion R_{AA} with and without nuclear shadowing effect at different rapidities, $b = 7.5$ fm.

jet distribution according to Eq. (6) at high transverse momentum which decreases faster than an overall power law, see Fig. 10.

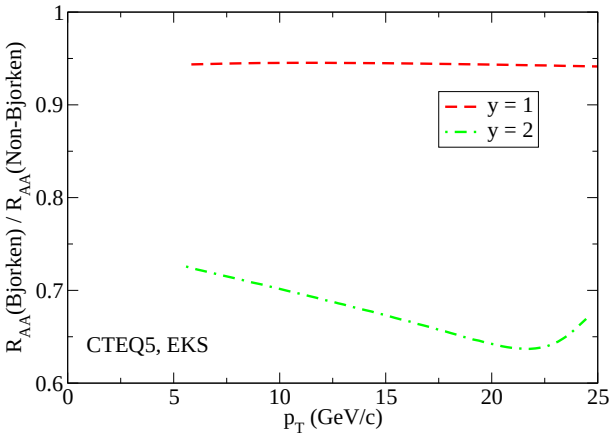

FIG. 13: (Color online) The ratio of the neutral pion R_{AA} imposing a boost-invariant expansion to R_{AA} as calculated from the 3D hydrodynamical (non-Bjorken) medium $b = 7.5$ fm.

One can also address the question how different the part of the medium is traversed by a jet which fragments into a pion at forward rapidity in comparison to one which fragments at midrapidity. We compare the full 3D hydrodynamical calculation to an effective 2D boost-invariant approach in which the 2D hydrodynamical solution at midrapidity is assumed to also describe the transverse profile at forward rapidity. This corresponds effectively to imposing *a posteriori* Bjorken expansion onto the non-Bjorken hydrodynamical evolution. We study the ratio of $R_{\rm AA}$ by imposing a boost invariant expansion, and comparing with the fully 3D non-Bjorken evolution. Fig. 13 shows a calculation at forward rapidities for non-central collisions with a finite impact parameter

of $b = 7.5$ fm. This ratio is obviously not measurable, but is interesting from a theoretical point of view. Its relatively strong deviations from 1 at $y = 2$ stem mainly from the different transverse temperature profiles at forward rapidity in the non-Bjorken evolution whereas these differences at $y = 1$ are not significant. The fact that the ratio is rather flat in p_T (it varies only in the range of 0.7 ± 0.05 for $y = 2$) indicates that the reduction of the quenching power of the medium in the non-Bjorken case compared to the boost-invariant one is similar for partons over the full range of initial jet energies probed in the collision. Therefore a measurement of the absolute normalization of R_{AA} at midrapidity and forward rapidities might be useful in quantifying the deviations arising from the simplifications made in boost invariant expansion models.

A. Dependence on Nuclear Parton Distribution Functions

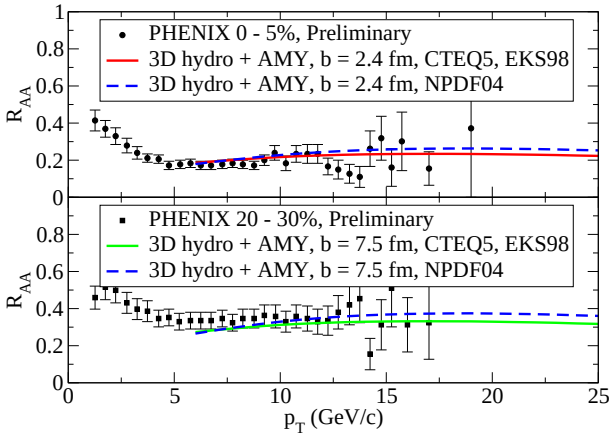

FIG. 14: (Color online) The neutral pion R_{AA} at midrapidity in most central (upper panel) and midperipheral (lower panel) Au+Au collisions compared with PHENIX data. Different prescriptions of nuclear parton distribution functions are used for comparison.

As has been pointed out earlier, see e.g. [48], the determination of nuclear parton distribution functions (nuclear PDFs) from experimental data is ambiguous. These uncertainties can also influence the calculation of the nuclear modification factor at mid and forward rapidity at RHIC. We compare in this subsections results obtained with the nuclear parton distribution functions as determined by NPDF04 [48] with those that were employed so far in this work, namely EKS98. We checked that the nucleon parton distributions which NPDF04 and EKS98 rely on, namely MRST01 and CTEQ5, respectively, lead to almost the same prediction of the inclusive cross section for π_0 production in $p + p$ collisions, cmp. Figs. 1 and 2. This should be expected since the determination

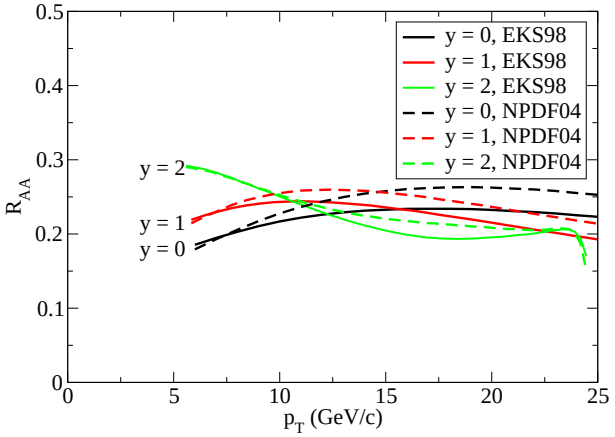

FIG. 15: (Color online) Comparing neutral pion R_{AA} at different rapidities using different descriptions of nuclear parton distribution functions, $b = 2.4$ fm.

of nucleon parton distribution functions has smaller uncertainties than those extended to nuclei.

Fig. 14 shows the neutral pion R_{AA} at midrapidity in central and midperipheral Au+Au collisions as obtained with the two different nuclear PDFs. Differences due to the different nuclear PDFs appear especially at larger transverse momenta of the produced pions. The same holds true for R_{AA} at forward rapidity, see Fig. 15 for a comparison in central collisions.

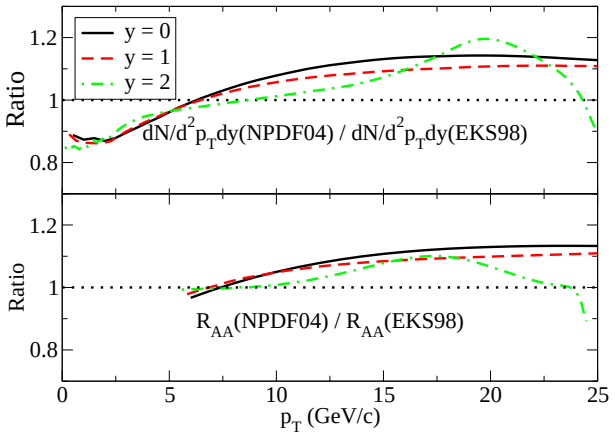

FIG. 16: (Color online) The ratio (NPDF04/EKS98) for the initial quark + anti-quark jet distributions (upper) and nuclear modification factors R_{AA} (lower) using different descriptions of nuclear parton distribution functions, $b = 2.4$ fm.

It is possible to trace these differences in R_{AA} back to differences in the initial jet distributions resulting mainly from the different shadowing descriptions. We show in Fig. 16 upper panel the ratio of the initial quark and anti-quark jet distributions as inferred from NPDF04 to EKS98. This translates - after jet-energy loss and fragmentation have been taken into account - into a similar

behavior of the ratios of the nuclear suppression factor R_{AA} in the two cases. Differences in the initial distribution (mainly resulting from different nuclear shadowing) will therefore be reflected in R_{AA} at mid and forward rapidity and at different centralities. Reduced sensitivity to differences in shadowing effects is expected if ratios of R_{AA} are considered: the ratio for $y = 1$ (Fig. 13) is only sensitive on the 1% level to employing EKS98 or NPDF04 (comparison not shown), the sensitivity for $y = 2$ is at most 4%. What we find in this subsection clearly demonstrate that that R_{AA} is not only sensitive to the employed jet quenching formalism but also to nuclear shadowing effects. The reason is that – even after energy loss and fragmentation – R_{AA} is sensitive to the initial jet distribution which in turn vary within the uncertainties of the determination of nuclear shadowing. A further reduction of uncertainties in the determination of nuclear shadowing effects will make a more stringent test of jet quenching formalisms by R_{AA} measurements.

V. CONCLUSIONS

In this paper, the jet energy loss was studied in the AMY-formalism using a 3D hydrodynamical evolution model that has been shown to describe the bulk properties of matter created in heavy-ion collisions at RHIC.

We have evaluated the nuclear suppression factor R_{AA} for neutral pions in central collisions as a function of p_T at mid and forward rapidity and have discussed how the azimuthal asymmetry of the medium in non-central collisions allows to put stronger constraints on our understanding of jet energy loss by gluon radiation. Since the jets probe different flow and temperature profiles in the asymmetric expansion depending on their initial positions and emission angles, R_{AA} is not only a function of p_T but also of the azimuth in those collisions.

The measured R_{AA} as a function of p_T in central and (averaged over the azimuth) in non-central collisions at midrapidity is in good agreement with the model calculations. We also have provided calculations of R_{AA} as a function of p_T and the azimuth without averaging that can be the basis of more stringent experimental tests once further data become available. We furthermore studied R_{AA} as a function of p_T in central and again averaged over the azimuth in non-central collisions at mid and forward rapidity and provided arguments that a measurement of these dependences might not only be able to reveal more information about the nuclear medium (as deviations from the assumption of boost invariance) but also provide a possibility to observe nuclear shadowing effects in the initial parton distribution function indirectly (assuming appropriate experimental resolution).

We emphasize that the description of R_{AA} (as a function of p_T, the azimuthal angle and rapidity) alone is not enough to prove the consistency of a specific energy loss mechanism with data, if assumptions about the medium evolution can be freely adjusted. On the contrary, R_{AA} will only provide stronger constraints on our theoretical physical conjectures about jet energy loss in the nuclear medium if studied in a dynamical evolution model which has been tested using soft observables.

VI. ACKNOWLEDGMENTS

It is a pleasure to thank S. Jeon and T. Renk for many discussions and comments. We thank W. Vogelsang for discussions. We thank Bryon Neufeld for computational assistance in extending our hydro-grid mapping routine to incorporate collective flow. C. G., G.-Y. Q., J. R., and S. T. acknowledge financial support by the Natural Sciences and Engineering Research Council of Canada. S. Bass acknowledges support by a grant from the U.S. Department of Energy (DE-FG02-03ER41239-0).

[1] K. Adcox *et al.* [PHENIX Collaboration], Phys. Rev. Lett. **88**, 022301 (2002).
[2] C. Adler *et al.* [STAR Collaboration], Phys. Rev. Lett. **89** 202301 (2002).
[3] M. Gyulassy and X. Wang, Nucl. Phys. **420** 583 (1994).
[4] R. Baier, Y. L. Dokshitzer, A. H. Mueller, S. Peigne and D. Schiff, Nucl. Phys. B **483** 291 (1997).
[5] M. Gyulassy, P. Levai and I. Vitev, Nucl. Phys. B **594**, 371 (2001)
[6] A. Kovner and U. A. Wiedemann, Review for Quark Gluon Plasma 3, Editors: R.C. Hwa and X.N. Wang, World Scientific, Singapore, 192 (2003), arXiv:hep-ph/0304151.
[7] B. G. Zakharov, JETP Lett. **63**, 952 (1996); JETP Lett. **65**, 615 (1997); JETP Lett. **70**, 176 (1999);
[8] X. N. Wang and X. f. Guo, Nucl. Phys. A **696** (2001) 788; A. Majumder, E. Wang and X. N. Wang, arXiv:nucl-th/0412061.
[9] P. Arnold, G. D. Moore and L. G. Yaffe, JHEP **0111**, 057 (2001); JHEP **0112**, 009 (2001); JHEP **0206**, 030 (2002).
[10] A. K. Dutt-Mazumder, J. e. Alam, P. Roy and B. Sinha, Phys. Rev. D **71** (2005) 094016.
[11] A. Adil, M. Gyulassy, W. A. Horowitz and S. Wicks, arXiv:nucl-th/0606010.
[12] M. G. Mustafa and M. H. Thoma, Acta Phys. Hung. A **22**, 93 (2005)
[13] X. N. Wang, arXiv:nucl-th/0604040.
[14] A. Dainese, C. Loizides and G. Paic, Eur. Phys. J. C **38** (2005) 461.
[15] A. Majumder, Phys. Rev. C **75**, 021901 (2007).
[16] T. Hirano and Y. Nara, Phys. Rev. C **66**, 041901 (2002).
[17] T. Renk and J. Ruppert, Phys. Rev. C **72**, 044901 (2005).
[18] T. Renk, Phys. Rev. C **70** (2004) 021903.
[19] C. A. Salgado and U. A. Wiedemann, Phys. Rev. D **68**, 014008 (2003).

[20] T. Renk and K. J. Eskola, arXiv:hep-ph/0610059.
[21] C. Nonaka and S. A. Bass, Phys. Rev. C **75**, 014902 (2007).
[22] T. Renk, J. Ruppert, C. Nonaka and S. A. Bass, arXiv:nucl-th/0611027.
[23] S. A. Bass, T. Renk, J. Ruppert and C. Nonaka, arXiv:nucl-th/0702079.
[24] A. Majumder, C. Nonaka and S. A. Bass, arXiv:nucl-th/0703019.
[25] T. Renk, arXiv:hep-ph/0608333.
[26] S. S. Adler *et al.* [PHENIX Collaboration], arXiv:nucl-ex/0611007.
[27] T. Renk and J. Ruppert, Phys. Rev. C **73** (2006) 011901
[28] T. Renk and J. Ruppert, arXiv:hep-ph/0702102.
[29] J. D. Bjorken, Phys. Rev. D **27**, 140 (1983).
[30] R. B. Clare and D. Strottman, Phys. Rept. **141**, 177 (1986).
[31] A. Dumitru and D. H. Rischke, Phys. Rev. C **59**, 354 (1999).
[32] P. F. Kolb, U. W. Heinz, P. Huovinen, K. J. Eskola and K. Tuominen, Nucl. Phys. A **696** (2001) 197.
[33] R. J. Fries, B. Muller, C. Nonaka and S. A. Bass, Phys. Rev. C **68**, 044902 (2003)
[34] C. W. De Jager, H. De Vries and C. De Vries, Atom. Data Nucl. Data Tabl. **14**, 479 (1974).
[35] H. L. Lai *et al.* [CTEQ Collaboration], Eur. Phys. J. C **12**, 375 (2000).
[36] K. J. Eskola, V. J. Kolhinen and C. A. Salgado, Eur. Phys. J. C **9**, 61 (1999).
[37] K. J. Eskola, H. Honkanen, H. Niemi, P. V. Ruuskanen and S. S. Rasanen, Phys. Rev. C **72**, 044904 (2005)
[38] B. Jäger, A. Schäfer, M. Stratmann and W. Vogelsang, Phys. Rev. D **67**, 054005 (2003)
[39] G. G. Barnafoldi, G. I. Fai, P. Levai, G. Papp and Y. Zhang, J. Phys. G **27**, 1767 (2001).
[40] S. S. Adler *et al.* [PHENIX Collaboration], arXiv:nucl-ex/0610036.
[41] S. Jeon and G. D. Moore, Phys. Rev. C **71**, 034901 (2005)
[42] S. Turbide, C. Gale, S. Jeon and G. D. Moore, Phys. Rev. C **72**, 014906 (2005).
[43] P. Aurenche, F. Gelis and H. Zaraket, JHEP **0205**, 043 (2002)
[44] B. A. Kniehl, G. Kramer and B. Potter, Nucl. Phys. B **582**, 514 (2000)
[45] http://www.phenix.bnl.gov/WWW/plots/show_plot.php ?editkey=p0439
[46] A. D. Martin, R. G. Roberts, W. J. Stirling and R. S. Thorne, Phys. Lett. B **531**, 216 (2002) [arXiv:hep-ph/0201127].
[47] J. Adams *et al.* [STAR Collaboration], Phys. Rev. Lett. **97**, 152302 (2006)
[48] M. Hirai, S. Kumano and T. H. Nagai, Phys. Rev. C **70**, 044905 (2004) [arXiv:hep-ph/0404093].
[49] Note that the energy loss in the hadronic medium is found to be subdominant in [22], while data indicate that it has to be assumed to be more significant in the higher twist formalism [24].